Journal of Fluorescence (2024) 34:1025–1037
https://doi.org/10.1007/s10895-023-03339-4

RESEARCH

Comparison of Selenic Acid and Pyruvic Acid-Loaded Silver Nanocarriers Impact on Colorectal Cancer Viability

Gökçe Erdemir[1,2] · Ferdane DANIŞMAN-KALINDEMIRTAŞ[3] · İshak Afşin KARIPER[4] · Dürdane Serap KURUCA[5] · Dilşad ÖZERKAN[6]

Received: 12 May 2023 / Accepted: 6 July 2023 / Published online: 13 July 2023
© The Author(s), under exclusive licence to Springer Science+Business Media, LLC, part of Springer Nature 2023, corrected publication 2023

Abstract

Colorectal cancer (CRC) is a leading cause of morbidity and death worldwide. As current cancer drugs are ineffective, new solutions are being sought in other fields, including nanoscience. Similarly, silver nanoparticles play an important role in the pharmaceutical industry as they act as anti-cancer agents with less harmful effects and are usually 1 to 100 nm in size. Selenic acid (SA) and pyruvic acid (PA) are involved in various metabolic pathways in cancer. For this reason, we decided to detect their influence on colorectal cancer using silver-based (Ag) nanocarriers. DLS, Zetasizer, SEM and UV-Vis analyses were used to characterize AgSA and AgPA. A UV spectrophotometer was used to analyze the release of the NPs. MTT analyses were used to measure the viability of HCT116 and HUVEC cells, and IC_{50} values were calculated using GraphPad Prism. The indicated dosage and particle size of AgSA NPs proved to be suitable for cytotoxicity. Moreover, injection of these nanoparticles into non-cancer cells proved safe due to their minimal toxicity. In contrast, the AgPA NPs have no cytotoxicity and induce proliferation of HCT116 cells. Finally, only the synthesised AgSA nanoparticles could be used for advanced cancer therapy, which is both inexpensive and has minimal side effects.

Keywords Silver nanoparticle · Pyruvic acid · Selenic acid · Cytotoxicity · Colorectal cancer

Introduction

The 3rd most frequent neoplasm and the 4th most prevalent reason for cancer-related deaths globally are colorectal cancer (CRC) [1]. Colorectal cancer (CRC) is expected to be extremely fatal in the next decades. Early-stage CRC can be treated with surgery and adjuvant therapy, but recurrence is common, and cancer drug resistance increases the likelihood of treatment failure [2]. Nanomaterials have become increasingly popular in biomedicine due to the advantages associated with their use; in particular, they have properties defined by dissolution and stability, they can be designed to improve their affinity by targeting cells, and they exhibit high levels of biocompatibility, low immune response, and minimal side effects [3, 4]. The role of nanomaterials in medical applications has gained importance. Therefore, in order to understand the principles of the action of nanomaterials at the molecular level, research must develop new concepts. As a result of their medical use, the synthesis and characterization of nanoparticles have gained importance. The nanoparticles have a limited range of structural changes, but their biological activity varies greatly due to the exposed

✉ Dilşad ÖZERKAN
dilsadokan@gmail.com

Ferdane DANIŞMAN-KALINDEMIRTAŞ
ferdanis@hotmail.com

1 Aziz Sancar Institute of Experimental Medicine and Research, Department of Molecular Medicine, Istanbul University, Istanbul, Turkey

2 Institute of Health Sciences, Istanbul University, Istanbul, Turkey

3 Faculty of Medicine, Department of Physiology, Erzincan Binali Yıldırım University, Erzincan, Turkey

4 Education Faculty, Department of Science Education, Erciyes University, Kayseri, Turkey

5 Faculty of Medicine, Department of Physiology, Istanbul Atlas University, İstanbul, Turkey

6 Faculty of Engineering and Architecture, Department of Genetic and Bioengineering, Kastamonu University, Kastamonu, Turkey

functional units on the surface of the particle [5]. The special properties of nanoparticles, such as their nanosize, huge surface-to-volume ratio and differences in the properties of surface atoms, draw attention to the implications of cancer prevention. The chemotherapeutic potential of metal-based anticancer drugs has been demonstrated in numerous malignancies but with a number of adverse effects. To avoid adverse effects of the drugs on normal cells, a pharmacology-friendly strategy needs to be proposed. Because of their high surface/volume ratio and reactivity, metallic and metal oxide nanostructures have a large potential effect. The synthesis of nanoparticles from several precious metals, including palladium, copper, silver and gold, has recently gained attention due to their unique properties and applications in various disciplines [6–8]. Green nanotechnology, on the other hand, can enable the fabrication of eco-friendly nanostructures with metals such as Zn, Ag, Au, Te and Pd using environmentally friendly and cost-effective methods based on the use of living organisms, natural biomolecules, and waste materials [9–13]. In addition, silver nanoparticles play a crucial role in pharmaceuticals as they act as antimicrobials that are less toxic and typically range in size from 1 to 100 nm [6–8, 14]. On the other hand, green synthesized silver nanoparticles have anticancer potential against various cancers such as lung cancer [15], colorectal cancer [16], leukaemia [17], liver cancer [18], etc.

Selenic acid has the formula H_2SeO_4 and is an inorganic chemical. It is a selenium oxo acid with the more precise structure $O_2Se(OH)_2$ [19]. Selenium is important for the chemical processes of plants and organisms and, as an antioxidant peptide, can help inhibit cell damage caused by free radicals [20]. Se compounds such as selenic acid are generally believed to exert antitumor properties primarily through their direct or indirect antioxidant abilities, which help maintain redox balance within the cell while protecting normal cells from damage caused by oxidation due to reactive oxygen species (ROS) [21, 22]. Selenium can be used to treat cancer, heart disease, rheumatoid arthritis and cystic fibrosis. Selenium oxygen anions can be dangerous to humans in high doses; however, their harmful effects are less when selenium is in its simplest form [23]. These selenium nanoparticles are characterized by having a small surface area per unit volume and high permeability, which increases their value while acting as ligands and increasing affinity on the way to their targets [24].

On the other hand, pyruvic acid (PA) is a smaller chemical molecule that is vital to the pharmaceutical, food, and agrochemical industries as well as to the metabolic processes of living things. PA is an end product of glucose oxidation in living organisms and is eventually converted to CO_2 and H_2O via the Krebs cycle. Since PA is involved in the metabolic process, it can serve as a biomarker for a variety of health conditions[25]. Kumar et al. (2015) synthesized SeNPs produced from the carboxyl group of pyruvic acid and showed antitumor activity against Dalton lymphoma cells (DL) [26].

In colorectal cancer, inhibiting the side effects of chemotherapeutic drugs is crucial for survival. Given the beneficial effects of SA and PA on cancer, in this study we wanted to search the impact of newly synthesized AgSA and AgPA NPs on inhibiting cell death in colorectal cancer. First, the NPs were characterized and their release was analyzed. Then, the cytotoxic experiments were performed on HCT16 and healthy HUVEC cells.

Materials and Methods

With regard to chemical compounds, Dulbecco's Modified Eagle's Medium (DMEM), MTT cell viability test kit, sodium borohydride ($NaBH_4$), silver nitrate $Ag(NO_3)$, and trisodium citrate (TSC) were purchased from Sigma Aldrich (St. Louis, USA), while DMSO, DMSO, and NaOH were obtained from Sigma Aldrich. Fetal bovine serum (FBS), penicillin, streptomycin, and trypsin were acquired from Gibco (UK), Gibco (USA), and Thermo Fisher (USA), respectively.

Synthesis of AgPA ve AgSA

Initially, stocks containing 4.3×10^{-3} M TSC, 2×10^{-3} M $NaBH_4$, and 1×10^{-3} M $Ag(NO_3)$ were created. At 60 °C for 30 min, 24 mL 1:1 (w/w) TSC/$NaBH_4$ was added. Then, 48 mL of $Ag(NO_3)$ was put in and the temperature of the solution was increased to 90 °C. The AgNPs stock solution was kept in an ark-cool atmosphere after its response ceased and a yellow color shift was seen.

The produced stock solutions of SA and PA were subsequently mixed in a 1:1 (w/w) ratio with AgNPs stock solutions. Both the drug and transport system was sonicated for thirty seconds at room temperature in an ultrasonic bath.

Characterization of AgPA ve AgSA

SA and PA binding to AgNPs was verified by zetasizer, DLS and SEM. The optical diffraction method was used to assess the AgSA and AgPA NPs size of particles. The Zetasizer Nano ZS (Malvern Instruments Ltd., Malvern, UK) equipped with a high-concentration zeta potential cell was used for the experiments presented in this study, which were carried out at 25 °C. The scattering of light was carried out at 25 °C and a 90°angle. With the use of an EVO40- LEO automated digitized scanning electron microscope (SEM), the AgSA and AgPA NPs surface characteristics were

examined. On conducting surfaces, the specimens were placed and allowed to dry. Liquid samples were placed onto copper wire electrodes prior to examination. After coating with Au/Pd, they were allowed to dry for 24 h before SEM examinations were carried out. The samples were characterized morphologically at a voltage of 25.00 KV and a magnification of 100.00 KV.

Distilled water was placed in the cell to the baseline beams and the Hach Lange 500 Spectrophotometer was used to take optical measurements at room temperature. The measurement's optical spectrum was captured at a wavelength in the 220–240 nm region (λmax: 230 nm) [27].

Drug Release Measurement

PBS buffer solutions with a pH of 7.4 and a dialysis membrane were used as media to measure the release of drugs placed on the nanocarrier. Separately, 1 mg/mL AgSA, AgPA were transferred to a 2 mL dialysis membrane. The diameter of the dialysis membrane is approximately 16 cm, and the ambient temperature is 37 ± 0.5 ºC. The dialysis membrane was sealed at both ends. The release of each drug from the NPs was monitored by adding them to 50 ml buffer solution containing SA and PA pH 7.4. Measurements at 390 nm in a UV spectrophotometer were performed at different time periods to analyze the release of PA and SA from the NPs [28, 29].

Cell Culture Experiments

HCT116 cancer cells and healthy HUVEC cells were grown in DMEM with 10% FBS and 1% pen/strep in this investigation. Incubation conditions were 37 °C, 95% humidity, and 5% CO_2 for the growth of HCT116 and HUVEC cells. The cells were trypsinized with 0.25% Trypsin-EDTA for passing and seeding each time after being rinsed with PBS and allowed to achieve 80% confluence.

Using an MTT test, the cytotoxic impact of AgPA and AgSA on HUVEC and HCT116 cells was assessed. Cell viability is measured using the MTT test. To ascertain the cytotoxic impact, the cells were grown at a density of 1×10^4 cells/100 µL of complete media in 96-well microplates. The trypan blue dye exclusion test was used to calculate the cell count. Different concentrations of PA, SA (5-20-100 M), and AgNPs (AgPA and AgSA) (0.2-2-10-20-50-100 µM) were applied to cells grown in DMEM. With 90 µl of cells in a complete medium and 10 µl/well added, each concentration was evaluated in triplicate. A 0.1% addition of DMSO was made to the control wells. For 72 h, the plates were incubated and after then, each well received 10 µl of MTT solution, which was then incubated for 4 h. In 100 µL of DMSO, formazan crystals were solubilized. A Rayto microplate reader was used to measure optical density at 560 nm with a 620 nm reference wavelength. The following calculation was used to calculate the viability % based on absorbance.

Viability (%) = (Mean absorbance of sample ÷ Mean absorbance of control) $x100$.

Hoechst Immunofluorescence Staining

We also wanted to demonstrate the effect of IC_{50} concentrations of PA, SA, AgPA, and AgSA on HCT116 cells with a fluorescent dye, Hoechst 33342. HCT116 cells were cultured in 96-well microplates as 8×10^3 cells/100 µL of complete medium per well. The IC_{90} concentrations of each compound were tested in triplicate using 10 µl/well added to the 90 µl of cells in a complete medium. Cell lines were maintained at 37 °C for 24 h while being exposed to 5% CO_2. The media were discarded after 24 h, followed by three cold PBS washes and a 3% glutaraldehyde fixation. The cell nuclei were stained for 15 min at room temperature with 10 µL of Hoechst (1 µg/mL), and then rinsed with PBS. Additionally, the samples underwent graded (30–100%) alcohol dehydration. Finally, the samples are stored in the dark at 4 °C until image analysis. The fluorescent images were taken at 385 nm via a Nikon microscope.

Statistical Analyzis

Data on cell viability were compared using GraphPad Prism 5.04 software and provided as mean SD for n = 3. Two different tests were used for statistical analysis of the data. The Mann-Whitney test was used to determine whether all doses of each group were significant compared to the control; the One-Way Anova test was used to determine the significance of all data sets among themselves. It was deemed important at $p < 0.05$.

Results

Characterization Results

The DLS and zeta potential data of AgNPs, AgSA and AgPA are shown in Figs. 1 and 2. Accordingly, the size of AgNPs generated ranged from 2.32 to 5.61 nm, while for AgSA it ranged from 3.61 to 13.54 nm. In contrast, particle sizes of 78.82 to 295.3 nm were observed for AgPA. This drop in zeta potential persisted and was measured to be -47.3 mV, -20.7 mV and − 7.31 mV for AgNPs, AgSA and AgPA, respectively. The conductivity of the solutions was also measured as 0.314 mS/m, 0.300 mS/cm and 0.270 mS/cm, respectively.

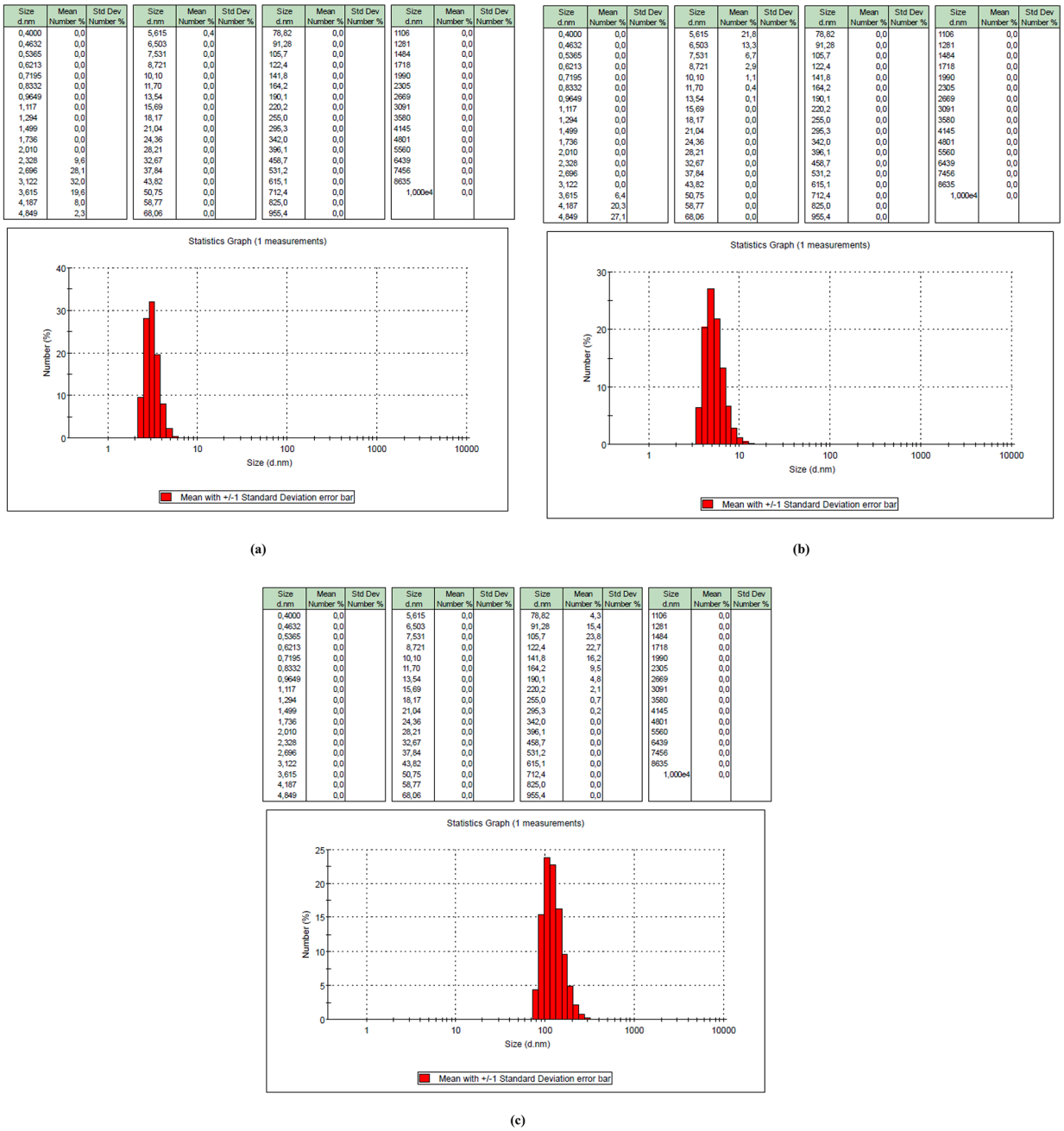

Fig. 1 DLS results of AgNPs (**a**), AgSA (**b**), AgPA (**c**)

The images showed that very small AgNPs and AgSA particles emerged below 100 nm. Particle growth may be seen in AgSA as opposed to AgNPs, despite the fact that there are accumulations brought on by caking when the solution dries. Again supporting the DLS findings, it was discovered that AgPA particles ranged in size from 100 to 200 nm (Fig. 3).

In addition to the Si, Na, Al elements originating from the base material, the Ag element, which is expected in AgNPs, was determined as 0.04% atomically, albeit low, and 0.02% in AgPA due to the excess of other components. The main reason for this is that carrier AgNPs are kept at very low concentrations while being synthesized. As a result of AgSA EDX, Se element originating from 0.62% selenoic acid was detected (Fig. 4).

The UV-VIS spectrum of the samples is given in Fig. 5. According to the literature, there is no known absorption peak in the 200–1100 nm range of the selenate anion [30].

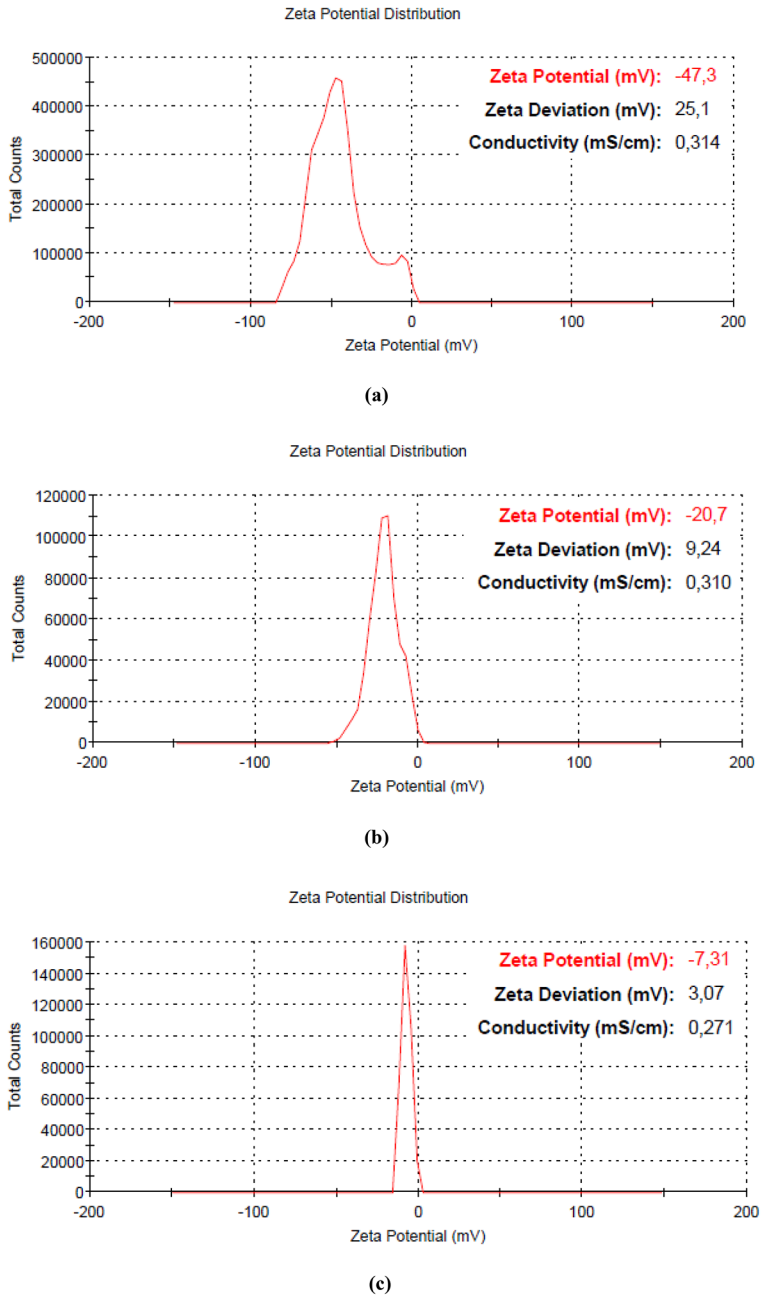

Fig. 2 Zeta Potential distribution of AgNPs (a), AgSA(b), AgPA(c)

It is well known in the literature that the pyruvate anion only gives an absorption peak in the pH: 1–4 range with a wavelength range of 200–1100 nm [31]. As it is known, since AgNPs have particle size around 400 nm and below 100 nm, specific absorption peak was observed [14]. On the other hand, depending on the size effect, AgSA absorption peaks at 398 nm and AgPA at 390 nm were observed. These results show that PA and SA are attached to the surface of AgNPs and AgNPs can be used as carriers.

Cumulative drug Release

To evaluate the drug release profile of the nanostructures, the release of PA and SA from SA and PA loaded Ag-based NPs was monitored at pH 7.4. According to the UV results of the prepared drug-loaded NPs, a gradual increase in the cumulative release value (%) over time was observed for each sample. After 48 h, SA reached 86.8% and PA reached 79% of the cumulative release rate (Fig. 6).

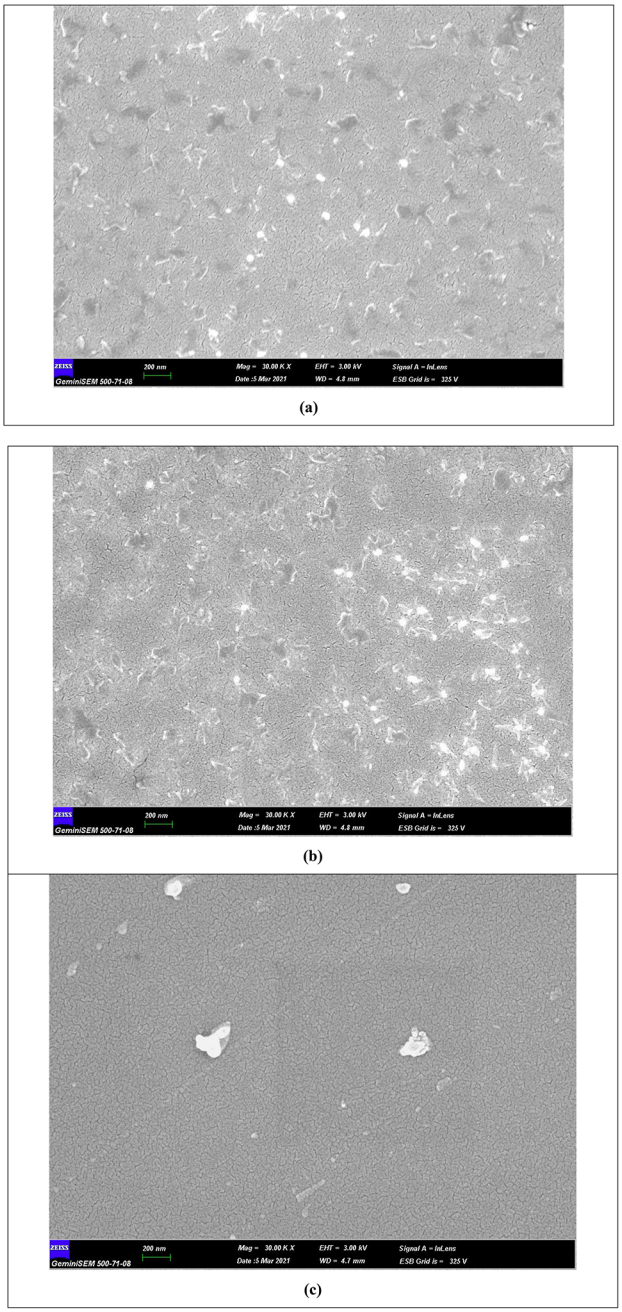

Fig. 3 AgNPs (**a**), AgSA (**b**), and AgPA (**c**) STEM pictures are shown

Cell Viability Analyzes

In Fig. 7, it is clearly seen that pyruvic acid is not cytotoxic effective on HCT116 and HUVEC cells; on the contrary, it increases the proliferation of these cells. In addition, although PA is loaded with silver nanoparticles, it does not appear to cause significant cytotoxicity in cells. In contrast to selenium, it is cytotoxic, with an IC_{50} value of 53 µg/mL in HCT116 cells and 100 µg/mL in HUVEC cells. In addition, loading SA onto silver nanoparticles has an IC_{50} value of 10 µg/mL, thus increasing the toxicity of HCT116 cells by 5.3 times (Table 1).

Morphologic Results

Figure 8 shows the morphological changes of HCT116 cells after incubation with PA, SA, AgPA, and AgSA according to their IC_{50} concentrations. Some cells appear to have much fewer intercellular connections and compromised cell

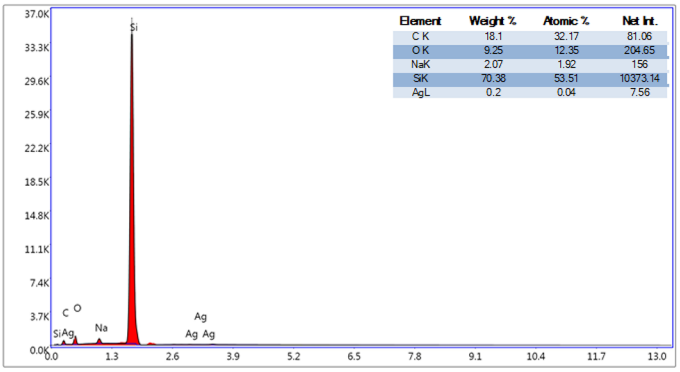

(a)

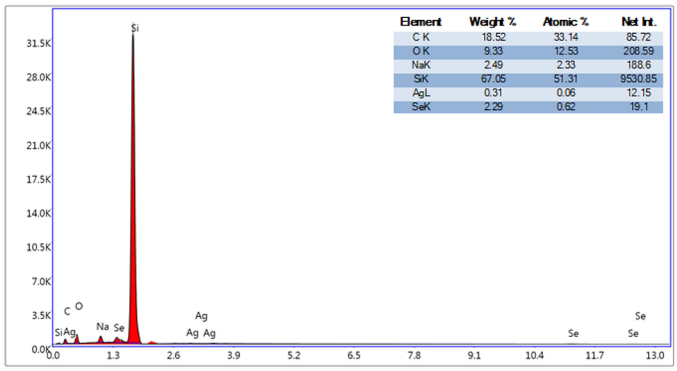

(b)

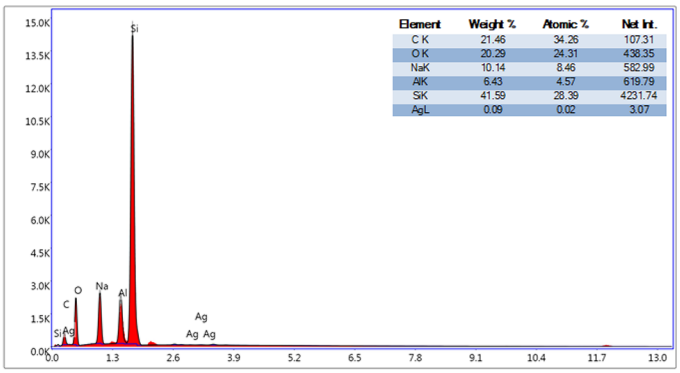

(c)

Fig. 4 EDX results for AgNPs, AgSA and AgPA are given

integrity after treatment. It is also interesting that the medication reduces cell confluence by around 50% when given to cancer cells. Nuclear fragmentation due to apoptotic death in some colonies and cell swelling due to necrotic death in other cell colonies were clearly visible with Hoechst staining in both the SA -treated and AgSA-treated HCT116 groups. On the other hand, the PA and AgPA groups did not have effective results in inhibiting cell viability. In contrast to the AgSA group, they induced cell proliferation at the same doses. The images taken with the inverted microscope are consistent with our findings on cytotoxicity.

Discussion

Nanotechnology involves the creation and use of materials and technologies at the atomic, molecular, cluster, and supramolecular levels, as well as their unique properties at the nanoscale [32]. Due to their unique properties, silver

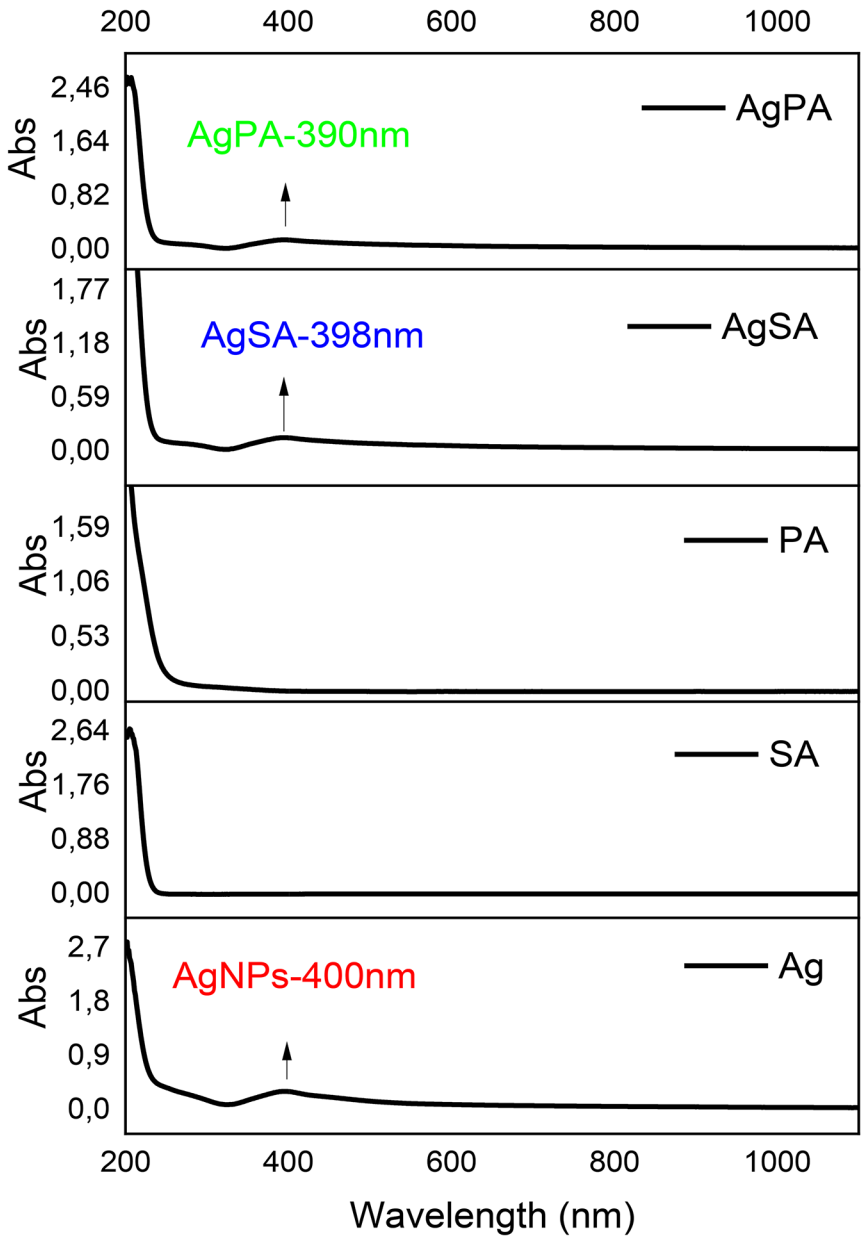

Fig. 5 UV-VIS spectrum of samples

nanoparticles (AgNPs) have recently shown therapeutic potential and are used as potent antimicrobial compounds with broad spectrum activity in textiles, food containers, antibacterial aerosols, catheters, dressings, and cancer prevention products [33]. DNA damage and chromosomal abnormalities are caused by low concentrations of AgNPs without causing significant cytotoxicity [34]. No genotoxic effects were observed in various cultured human cells exposed to at least 10 mg/mL of encapsulated AgNPs with a mean diameter of 6–80 nm. AgNPs have been shown to interact with cells, regulating numerous cellular responses both passively and actively [35]. According to the literature, it has been understood that drug systems with small particle sizes are more likely to enter the cell, as well as the negative side of surface potentials has a better effect on cancer cells [36]. There are also factors that may have an impact on the biological activity of inorganic nanoparticles. These factors include size distribution, morphology, surface charge, surface chemistry, capping agents, etc. [8, 17, 18].

By inhibiting the phosphorylation stage of protein kinase -Akt, AgNPs' anti-angiogenic action in vascular endothelial cells has been demonstrated to be equal to that of a naturally occurring anti-angiogenic compound identified as a pigmented epithelium-derived factor [37]. It was also shown that the mouse cancer model might potentially be toxic to Dalton's Lymphoma Ascites (DLA) and DLA-induced

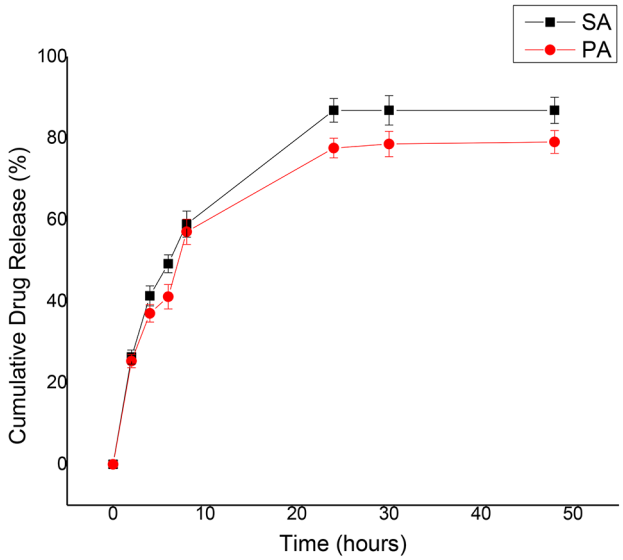

Fig. 6 Graph of cumulative drug release of SA and PA from AgPA and AgSA over time

Table 1 The effect of PA, SA, AgPA, and AgSA on HUVEC and HCT116 cell lines. Proliferation was evaluated by MTT. IC_{50} values were taken after 72 h

* IC_{50} (μg/ml): Concentration that inhibited cell growth by 50%

	PA	SA	AgPA	AgSA
HUVEC	> 100 μg/mL	100 μg/mL	> 100 μg/mL	19 μg/mL
HCT116	> 100 μg/mL	53 μg/mL	> 100 μg/mL	10 μg/mL

tumors, with considerably longer surviving time in comparison to the control group [38]. Low amounts of poly(N-vinyl-2-pyrrolidone)-coated AgNPs reduced the viability of acute myeloid leukemia cells and K562 cells following infiltrating the cells through the route of endocytic endosomes in a dose-dependent way [39]. In addition, AgNPs were shown to have cytotoxic effects on cancer cells and to exert anticarcinogenic properties. These effects included triggering cell death via intrinsic and extrinsic pathways against a variety of carcinoma cell types, including human breast cancer cell lines (MCF −7, MDA-MB -231), lung cancer cell lines (A549), liver cell lines (HepG2), and skin and oral cavity carcinoma cell lines (HT144), by leaking lactate levels [40–42]. Even so, a variety of factors,

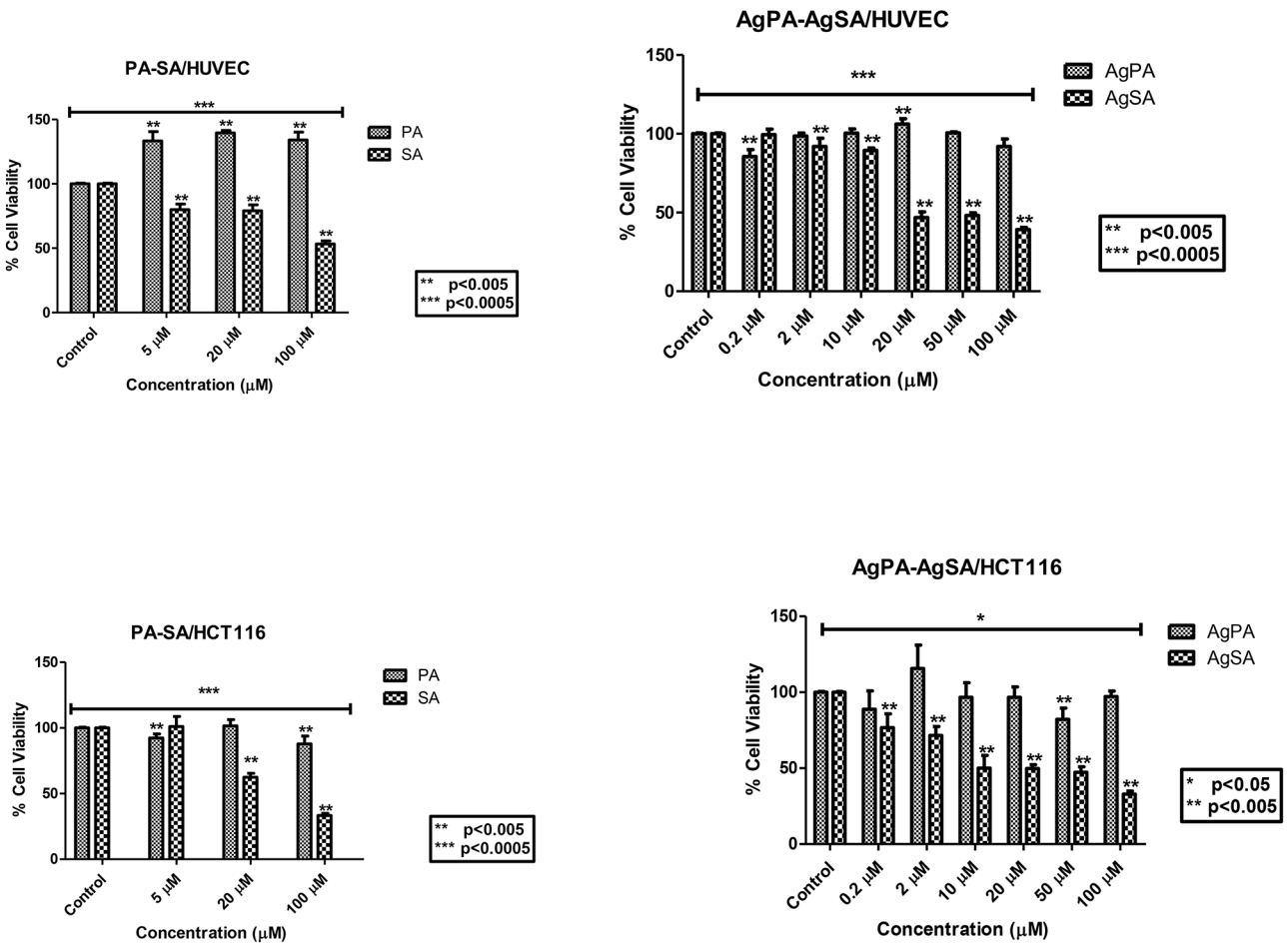

Fig. 7 Viability (%) of HUVEC and HCT116 cells incubated in various PA, SA, AgPA, and AgSA concentrations for 72 h

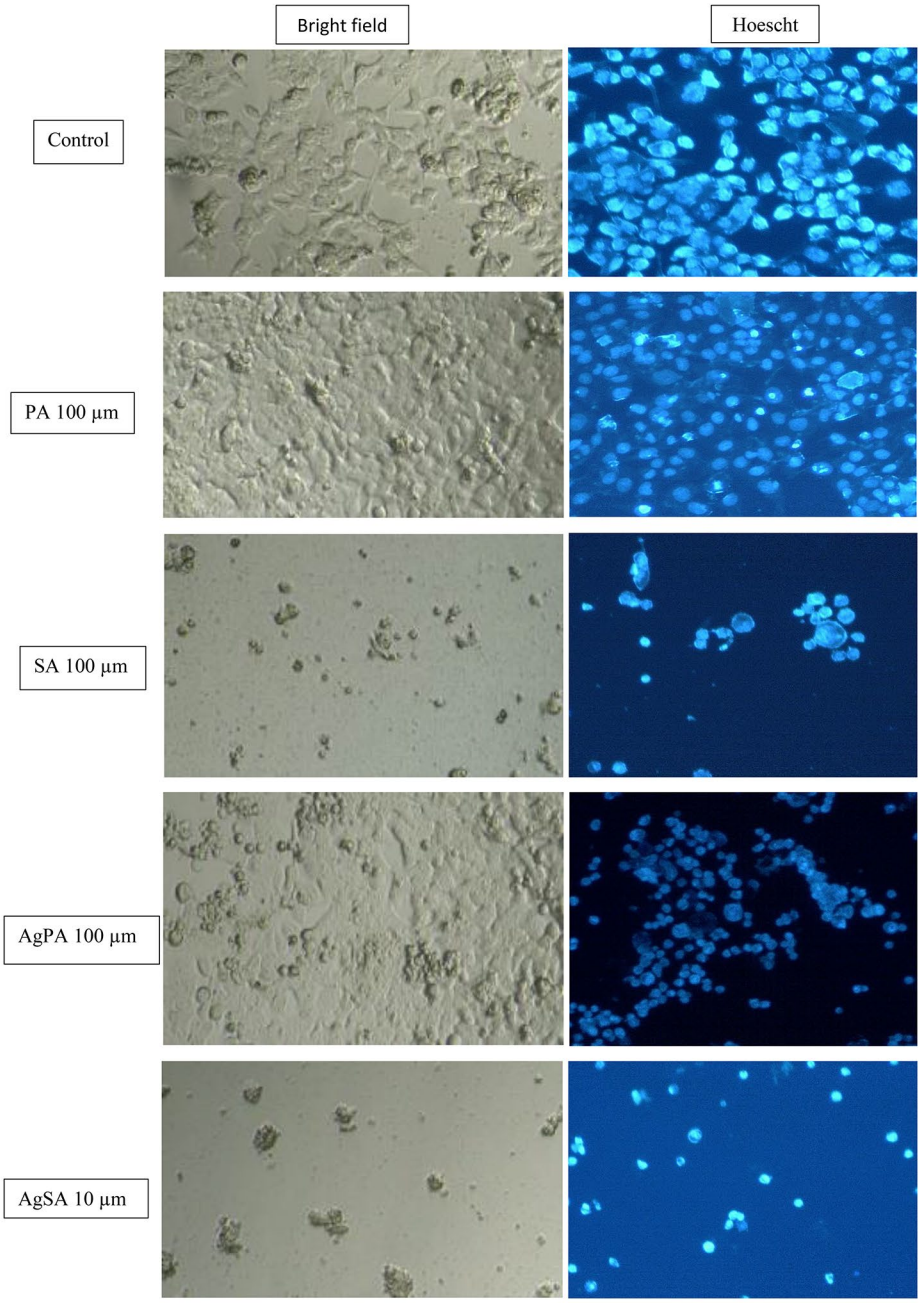

Fig. 8 HCT116 cells after incubation in PA, SA, AgPA, and AgSA proper concentrations and times. Magnification: x100

including AgNPs' shape, size, and surface coatings, as well as the charge on their surfaces, the kind of cells employed, and the anti-cancer chemicals used to produce them, affect their anti-cancer activities. Despite the fact that conventional chemical and physical methods are straightforward, they use a lot of energy and dangerous substances [42]. In addition to harmful and non-renewable, artificial covering agents such as polyethylene glycol, polyvinylpyrrolidone, and polyvinyl alcohol. As a result, the demand for AgNP coatings made from macromolecules is increasing.

Due to its low toxicity, selenium is a vital element that has excellent cancer preventive and inhibitory properties [43]. In this regard, dietary supplementation with lower side effects, such as selenium-based treatment, seems to be a possible strategy. The major crystalline form of selenium is a trigonal form with spiral chains, followed by a monoclinic form with Se8 rings, which is less stable [20]. There are three different types of monoclinic Se, and each has a different ring configuration [20, 21]. Different disordered chains form crystalline selenium. Se is an effective antitumor

molecule by itself, but the selenium-added AgNPs may increase the effective diversity of its anticancer behavior. An intermediate in the breakdown of lipids, carbohydrates, and proteins is pyruvic acid. The Krebs cycle ends with the degradation of carbohydrates to pyruvic acid, which is degraded to CO_2 and H_2O in subsequent stages. This suggests that the Krebs cycle is the primary mechanism for energy production as long as oxygen is present PA. However, in the absence of oxygen, PA is involved in the fermentation of lactic acid [44, 45]. Based on the finding that resected GBM have increased lactate content (LA), Lu et al. 2022 mimicked pharmaceutical NPs that transport drugs for synergistic treatment based on LA metabolism. They can target GBM because their self-assembling NPs, which are encased in membranes produced from glioma cells, may easily traverse the blood-brain barrier. Before LA reaches the tumors, lactate oxidase in the NPs transforms it to PA and hydrogen peroxide. They found that PA inhibits the growth of cancer cells by halting histone expression and inducing cell cycle arrest [46]. In this study, we stabilized AgNPs by adding SA and PA The sizes of AgSA and AgPA NPs were found to be in suitable diameters and shapes for the treatment of HCT116 cells. Comparing AgSA with AgPA NPs, it can be said that AgSA is a successful candidate for the treatment of colorectal cancer as it is cytotoxic at lower doses and non-toxic to healthy cells. In contrast, Ag nanostructures loaded with PA showed no remarkable toxicity to HCT116 cells. In fact, the doses used with these cells were observed to increase proliferation. The release potential of AgSA also proved to be suitable for tumor region penetration. When all these results are evaluated together, AgSA could be used as an anti-cancer drug.

Conclusion

We have used SA and PA to stabilize and minimize the metal toxicity of AgNPs to circumvent the limitations of current approaches and generate AgNPs with effective structural and physical properties for physiological use in humans. There is limited research that has addressed the degradation of silver to produce AgNPs. In this work, we thoroughly investigated the anticancer properties of AgSA and AgPA NPs using human colorectal cancer cell line HCT116. The results show that the selenic acid-based AgNPs inhibit cancer cell viability. In contrast, AgPA NPs is not suitable candidate for colorectal cancer. Therefore, advanced cancer therapy with the synthesized AgSA could be cost-effective and have fewer side effects.

Author Contributions G.E did cell culture analyses, F.D.K. found the concept, İ.A.K. did the synthesizing and characterization of AgNPs, D.S.K. statistical analyzes, D.Ö. and F.D.K wrote the main manuscript text.

Funding There is no funding.

Data Availability Graphpad datasets are available.

Declarations

Competing Interests The authors declare no competing interests.
Ethical Approval.
Ethics committee approval is not required as the cell lines used are commercially available.
Competing interests.
Not Applicable.

References

1. Navarro M, Nicolas A, Ferrandez A, Lanas A (2017) Colorectal cancer population screening programs worldwide in 2016: an update. World J Gastroenterol 23:3632. https://doi.org/10.3748/WJG.V23.I20.3632
2. Hossain MS, Karuniawati H, Jairoun AA et al (2022) Colorectal Cancer: a review of Carcinogenesis, Global Epidemiology, Current Challenges, risk factors, preventive and treatment strategies. Cancers (Basel) 14. https://doi.org/10.3390/CANCERS14071732
3. Garbo S, Maione R, Tripodi M, Battistelli C (2022) Next RNA therapeutics: the mine of non-coding. Int J Mol Sci 23. https://doi.org/10.3390/IJMS23137471
4. Danışman-Kalındemirtaş F, Kariper İA, Erdemir G et al (2022) Evaluation of anticancer effects of carboplatin–gelatin nanoparticles in different sizes synthesized with newly self-assembly method by exposure to IR light. Sci Rep 2022 12(1 12):1–11. https://doi.org/10.1038/s41598-022-15051-7
5. Kumar M, Dwivedi C, Shah CP et al (2011) An organic acid-induced synthesis and characterization of selenium nanoparticles. J Nanotechnol. https://doi.org/10.1155/2011/651971
6. Yaqoob AA, Umar K, Ibrahim MNM (2020) Silver nanoparticles: various methods of synthesis, size affecting factors and their potential applications–a review. Appl Nanosci (Switzerland) 10:1369–1378. https://doi.org/10.1007/S13204-020-01318-W/FIGURES/5
7. Barabadi H (2017) Nanobiotechnology: a promising scope of gold biotechnology. Cell Mol Biol 63:3–4. https://doi.org/10.14715/10.14715/CMB/2017.63.12.2
8. Virmani I, Sasi C, Priyadarshini E et al (2020) Comparative anticancer potential of biologically and chemically synthesized gold nanoparticles. J Clust Sci 31:867–876. https://doi.org/10.1007/S10876-019-01695-5/FIGURES/10
9. Vahidi H, Kobarfard F, Alizadeh A et al (2021) Green nanotechnology-based tellurium nanoparticles: exploration of their antioxidant, antibacterial, antifungal and cytotoxic potentials against cancerous and normal cells compared to potassium tellurite. Inorg Chem Commun 124:108385. https://doi.org/10.1016/J.INOCHE.2020.108385
10. Cruz DM, Mostafavi E, Vernet-Crua A et al (2020) Green nanotechnology-based zinc oxide (ZnO) nanomaterials for biomedical applications: a review. J Physics: Mater 3:034005. https://doi.org/10.1088/2515-7639/AB8186
11. Samir N et al (2023) Dilşad Özerkan ·, Ferdane Danışman-Kalındemirtaş ·, Synthesis and Anticancerogenic Effect of New Generation Ruthenium-Based Nanoparticle from Homalothecium sericeum with Eco-Friendly Method. Journal of

Pharmaceutical Innovation 2023 1–12. https://doi.org/10.1007/S12247-023-09725-6
12. Honary S, Barabadi H, Ebrahimi P et al (2015) Development and optimization of Biometal Nanoparticles by using Mathematical Methodology: a Microbial Approach. J Nano Res 30:106–115. https://doi.org/10.4028/WWW.SCIENTIFIC.NET/JNANOR.30.106
13. Barabadi H, Webster TJ, Vahidi H et al (2020) Green Nanotechnology-based gold nanomaterials for hepatic Cancer therapeutics: a systematic review. Iran J Pharm Res 19:3–17. https://doi.org/10.22037/IJPR.2020.113820.14504
14. Danışman-Kalındemirtaş F, Kariper A, Hepokur C, Erdem-Kuruca S (2021) Selective cytotoxicity of paclitaxel bonded silver nanoparticle on different cancer cells. J Drug Deliv Sci Technol 61:102265. https://doi.org/10.1016/J.JDDST.2020.102265
15. Barabadi H, Hosseini O, Damavandi Kamali K et al (2020) Emerging Theranostic Silver Nanomaterials to combat Lung Cancer: a systematic review. J Clust Sci 31:1–10. https://doi.org/10.1007/S10876-019-01639-Z(
16. Barabadi H, Vahidi H, Damavandi Kamali K et al (2019) Emerging Theranostic Silver Nanomaterials to combat colorectal Cancer: a systematic review. J Clust Sci 31:311–321. https://doi.org/10.1007/S10876-019-01668-8
17. Mostafavi E, Zarepour A, Barabadi H et al (2022) Antineoplastic activity of biogenic silver and gold nanoparticles to combat leukemia: beginning a new era in cancer theragnostic. Biotechnol Rep 34:e00714. https://doi.org/10.1016/J.BTRE.2022.E00714
18. Barabadi H, Vahidi H, Rashedi M et al (2020) Recent advances in biological mediated cancer research using silver nanoparticles as a promising strategy for hepatic cancer therapeutics: a systematic review. Nanomed J 7:251–262. https://doi.org/10.22038/NMJ.2020.07.00001
19. Ullmann's Encyclopedia of Industrial Chemistry
20. Yu B, You P, Song M et al (2016) A facile and fast synthetic approach to create selenium nanoparticles with diverse shapes and their antioxidation ability. New J Chem 40:1118–1123. https://doi.org/10.1039/C5NJ02519B
21. Tan HW, Mo HY, Lau ATY, Xu YM (2018) Selenium Species: current status and potentials in Cancer Prevention and Therapy. Int J Mol Sci 20. https://doi.org/10.3390/IJMS20010075
22. Shi Z, Liu J, Tian L et al (2022) Insights into stimuli-responsive diselenide bonds utilized in drug delivery systems for cancer therapy. Biomed Pharmacother 155:113707. https://doi.org/10.1016/J.BIOPHA.2022.113707
23. Nayak V, Singh KR, Singh AK, Singh RP (2021) Potentialities of selenium nanoparticles in biomedical science. New J Chem 45:2849–2878. https://doi.org/10.1039/D0NJ05884J
24. Jain R, Dominic D, Jordan N et al (2016) Higher cd adsorption on biogenic elemental selenium nanoparticles. Environ Chem Lett 14:381–386. https://doi.org/10.1007/S10311-016-0560-8/TABLES/2
25. Dsouza Priya Swetha P, Sudhakara Prasad K (2020) A non-enzymatic Disposable Electrochemical Sensor for Pyruvic Acid. Electroanalysis 32:2237–2243. https://doi.org/10.1002/ELAN.202060206
26. Kumar S, Tomar MS, Acharya A (2015) Carboxylic group-induced synthesis and characterization of selenium nanoparticles and its anti-tumor potential on Dalton's lymphoma cells. Colloids Surf B Biointerfaces 126:546–552. https://doi.org/10.1016/J.COLSURFB.2015.01.009
27. Kesharwani P, Kumar Tekade R, Jain NK et al (2011) Spectrophotometric estimation of paclitaxel combination drug and gene therapy using nanoparticles View project drug delivery view project Spectrophotometric estimation of paclitaxel. Article in International Journal of Advances in Pharmaceutical Sciences 2:29–32
28. Singh N, Saha P, Rajkumar K, Abraham J Biosynthesis of silver and selenium nanoparticles by Bacillus sp. JAPSK2 and evaluation of antimicrobial activity
29. Anthon GE, Barrett DM (2003) Modified method for the determination of pyruvic acid with dinitrophenylhydrazine in the assessment of onion pungency. J Sci Food Agric 83:1210–1213. https://doi.org/10.1002/JSFA.1525
30. Matai I, Pandey SK, Garg D et al (2020) Phytogreen synthesis of multifunctional nano selenium with antibacterial and antioxidant implications. Nano Express 1:010031. https://doi.org/10.1088/2632-959X/AB8BEA
31. Shemesh D, Luo M, Grassian VH, Gerber RB (2020) Absorption spectra of pyruvic acid in water: insights from calculations for small hydrates and comparison to experiment. Phys Chem Chem Phys 22:12658–12670. https://doi.org/10.1039/D0CP01810D
32. Moharramnejad M, Ehsani A, Shahi M et al (2023) MOF as nanoscale drug delivery devices: synthesis and recent progress in biomedical applications. J Drug Deliv Sci Technol 81:104285. https://doi.org/10.1016/J.JDDST.2023.104285
33. De Matteis V, Cascione M, Toma CC, Leporatti S (2018) Silver Nanoparticles: Synthetic Routes, In Vitro Toxicity and Theranostic Applications for Cancer Disease. Nanomaterials 2018, Vol 8, Page 319 8:319. https://doi.org/10.3390/NANO8050319
34. Ferdous Z, Nemmar A (2020) Health Impact of Silver Nanoparticles: a review of the Biodistribution and Toxicity following various routes of exposure. Int J Mol Sci 21. https://doi.org/10.3390/IJMS21072375
35. de Lima R, Seabra AB, Durán N (2012) Silver nanoparticles: a brief review of cytotoxicity and genotoxicity of chemically and biogenically synthesized nanoparticles. J Appl Toxicol 32:867–879. https://doi.org/10.1002/JAT.2780
36. Danişman-Kalindemirtaş F, Özerkan D, Kariper İA, Bulut H (2023) The Novel 5-Fluorouracil Loaded Ruthenium-based Nanocarriers enhanced anticancer and apoptotic efficiency while reducing Multidrug Resistance in Colorectal Cancer cells. J Fluoresc. https://doi.org/10.1007/S10895-023-03180-9
37. Gurunathan S, Lee KJ, Kalishwaralal K et al (2009) Antiangiogenic properties of silver nanoparticles. Biomaterials 30:6341–6350. https://doi.org/10.1016/J.BIOMATERIALS.2009.08.008
38. Irulappan Sriram M, Barath Mani Kanth S, Kalishwaralal K et al (2010) Antitumor activity of silver nanoparticles in Dalton's lymphoma ascites tumor model. Int J Nanomedicine 5:753–762. https://doi.org/10.2147/IJN.S11727
39. Guo D, Zhu L, Huang Z et al (2013) Anti-leukemia activity of PVP-coated silver nanoparticles via generation of reactive oxygen species and release of silver ions. Biomaterials 34:7884–7894. https://doi.org/10.1016/J.BIOMATERIALS.2013.07.015
40. Sahu S, Sinha N, Bhutia SK et al (2014) Luminescent magnetic hollow mesoporous silica nanotheranostics for camptothecin delivery and multimodal imaging. J Mater Chem B 2:3799–3808. https://doi.org/10.1039/C3TB21669A
41. Jagannath CV, POTENTIATION OF ANTIEPILEPTIC ACTIVITY OF PHENYTOIN USING BETA CAROTENE AGAINST MAXIMAL ELECTROSHOCK INDUCED CONVULSIONS IN MICE (2017) World J Pharm Pharm Sci 1574–1585. https://doi.org/10.20959/WJPPS20174-8945
42. Gurunathan S, Jeong JK, Han JW et al (2015) Multidimensional effects of biologically synthesized silver nanoparticles in Helicobacter pylori, Helicobacter felis, and human lung (L132) and lung carcinoma A549 cells. Nanoscale Res Lett 10:1–17. https://doi.org/10.1186/S11671-015-0747-0
43. Zeebaree SYS, Zeebaree AYS, Zebari OIH (2020) Diagnosis of the multiple effect of selenium nanoparticles decorated by Asteriscus graveolens components in inhibiting HepG2 cell proliferation. Sustain Chem Pharm 15:100210. https://doi.org/10.1016/J.SCP.2019.100210

44. Li YS, Ju X, Gao XF et al (2008) Immobilization enzyme fluorescence capillary analysis for determination of lactic acid. Anal Chim Acta 610:249–256. https://doi.org/10.1016/J.ACA.2008.01.049
45. Huang Y, Tian Y, Zhang Z, Peng C (2012) A HILIC–MS/MS method for the simultaneous determination of seven organic acids in rat urine as biomarkers of exposure to realgar. J Chromatogr B 905:37–42. https://doi.org/10.1016/J.JCHROMB.2012.07.038
46. Lu G, Wang X, Li F et al (2022) Engineered biomimetic nanoparticles achieve targeted delivery and efficient metabolism-based synergistic therapy against glioblastoma. Nature Communications 2022 13:1 13:1–17. https://doi.org/10.1038/s41467-022-31799-y

Publisher's Note Springer Nature remains neutral with regard to jurisdictional claims in published maps and institutional affiliations.

Springer Nature or its licensor (e.g. a society or other partner) holds exclusive rights to this article under a publishing agreement with the author(s) or other rightsholder(s); author self-archiving of the accepted manuscript version of this article is solely governed by the terms of such publishing agreement and applicable law.